The fungal metabolite 4-hydroxyphenylacetic acid from Neofusicoccum parvum modulates defence responses in grapevine

Noemi Flubacher, Raymonde Baltenweck, Philippe Hugueney, Jochen Fischer, Eckhard Thines, Michael Riemann, Peter Nick, Islam M Khattab

Received: 2 February 2023 | Revised: 28 June 2023 | Accepted: 4 July 2023

DOI: 10.1111/pce.14670

ORIGINAL ARTICLE

Plant, Cell & Environment WILEY

The fungal metabolite 4-hydroxyphenylacetic acid from *Neofusicoccum parvum* modulates defence responses in grapevine

Noemi Flubacher[1] | Raymonde Baltenweck[2] | Philippe Hugueney[2] | Jochen Fischer[3] | Eckhard Thines[3] | Michael Riemann[1] | Peter Nick[1] | Islam M. Khattab[1,4,5]

[1]Department of Molecular Cell Biology, Joseph Gottlieb Kölreuter Institute of Plant Science, Karlsruhe Institute of Technology, Karlsruhe, Germany

[2]INRAE, SVQV UMR-A 1131, Université de Strasbourg, Colmar, France

[3]Institut für Biotechnologie und Wirkstoff-Forschung gGmbH, Mainz, Germany

[4]Institute for Biological Interfaces 5, Karlsruhe Institute of Technology, Karlsruhe, Germany

[5]Department of Horticulture, Faculty of Agriculture, Damanhour University, Damanhour, Egypt

Correspondence
Noemi Flubacher, Fritz-Haber-Weg 4, 76131 Karlsruhe, Germany.
Email: noemi.flubacher@kit.edu

Funding information
Deutscher Akademischer Austausch Dienst GERLS Programme; European Regional Development Fund; Karlsruhe Institute of Technology

Abstract

In a consequence of global warming, grapevine trunk diseases (GTDs) have become a pertinent problem to viticulture, because endophytic fungi can turn necrotrophic upon host stress killing the plant. In *Neofusicoccum parvum* Bt-67, plant-derived ferulic acid makes the fungus release Fusicoccin aglycone triggering plant cell death. Now, we show that the absence of ferulic acid lets the fungus secrete 4-hydroxyphenylacetic acid (4-HPA), mimicking the effect of auxins on grapevine defence and facilitating fungal spread. Using *Vitis* suspension cells, we dissected the mode of action of 4-HPA during defence triggered by the bacterial cell-death elicitor, harpin. Early responses (cytoskeletal remodelling and calcium influx) are inhibited, as well as the expression of *Stilbene Synthase 27* and phytoalexin accumulation. In contrast to other auxins, 4-HPA quells transcripts for the auxin conjugating GRETCHEN HAGEN 3. We suggest that 4-HPA is a key component of the endophytic phase of *N. parvum* Bt-67 preventing host cell death. Therefore, our study paves the way to understand how GTDs regulate their latent phase for successful colonisation, before turning necrotrophic and killing the vines.

KEYWORDS
4-hydroxyphenylacetic acid, auxin, grapevine trunk disease, *Neofusicoccum parvum*, piceatannol, *Vitis vinifera*

1 | INTRODUCTION

Grapevine trunk diseases (GTDs), such as *Botryosphaeriaceae*-related Dieback (BD), have become a major threat for viticulture during the past decades, causing economic damage for the industry by loss of yield and replacement costs of globally at least 1.5 billion US$ per year (Hofstetter et al., 2012). Just for BD alone yield losses in 'Cabernet Sauvignon' reached to more than 45% for the harvesting season 2018–2019 (Larach et al., 2020). The frequency of GTD outbreaks has increased in parallel to extreme weather conditions following climate change (Galarneau et al., 2019; Slippers & Wingfield, 2007). Pathogenic pressure and symptoms caused by *Botryosphaeriaceae* often follow other stresses like drought (Blodgett et al., 1997; Desprez-Loustau

et al., 2006), a phenomenon also observed for other GTD-associated fungi (Sosnowski et al., 2011).

BD differs from classical pathogenesis as the fungus can live several years endophytically without causing symptoms, before suddenly turning pathogenic by switching to a necrotrophic lifestyle, such that the host is killed within a few days entirely or partially, by dieback of individual branches (Bertsch et al., 2013; Blodgett et al., 1997; Schoeneweiss 1981; Slippers & Wingfield, 2007). A slow or chronic form of the disease (latent state of BD) with inconsistently expressed symptoms has also been described, weakening the plant progressively (Bertsch et al., 2013; Slippers & Wingfield, 2007; Úrbez-Torres, 2011). Characteristic symptoms of BD are discoloration, root and shoot dieback, as well as foliar symptoms referred to as "tiger stripes" (Bertsch et al., 2013; Úrbez-Torres, 2011). Since the endophytic phase lacks any obvious symptoms, early-phase infections are often overlooked (Slippers & Wingfield, 2007).

Among the various *Botryosphaeriaceae*-species associated with symptomatic outbreaks of BD (Mondello et al., 2018; Reis et al., 2016; Úrbez-Torres & Gubler, 2009), *Neofusicoccum parvum* and the isolate Bt-67 in particular, is described as very aggressive, such that it is suited as experimental model for studies on host–pathogen interaction (Leal et al., 2021; Trotel-Aziz et al., 2019; Trotel-Aziz et al., 2022).

The complex molecular mechanism of interaction and chemical communication between *N. parvum* and *Vitis* are not completely unravelled yet. Based on previous studies, an interaction model was established, postulating the ability of *N. parvum* to change its behaviour depending on the physiological state of the host by selective release of fungal compounds (Khattab et al., 2021; Khattab et al., 2022). Under (drought) stress, the plant monolignol precursor ferulic acid accumulates. This compound is used by *N. parvum* as a "surrender signal" reporting that its host is under severe stress and, thus, a fungal change is needed to finalise its life cycle. In fact, ferulic acid was identified as a specific activator triggering the release of the fungal phytotoxin Fusicoccin A (FCA), an efficient trigger of programmed cell death (PCD) (Khattab et al., 2021; Khattab et al., 2022). This chemical exchange of information, possibly also including further fungal metabolites (Abou-Mansour et al., 2015; Ramírez-Suero et al., 2014; Salvatore et al., 2021; Trotel-Aziz et al., 2022), between the stressed host and the so far endophytic and not yet pathogenic fungus marks the transition towards apoplexy and the outbreak of *N. parvum*-induced BD symptoms *in planta* (Khattab et al., 2022).

Whether it is just the absence of the signalling circuit constituted by ferulic acid and FCA that sustains the long-lasting endophytic phase, or whether the endophytic lifestyle with host colonisation of the fungus is enabled by a different signal, has remained unknown.

Interestingly, when not challenged with ferulic acid, fungal cultures secrete 4-hydroxyphenylacetic acid (4-HPA) (Khattab et al., 2022). This phenolic metabolite is structurally similar to known compounds belonging to the auxins. While in the synthetic auxin 1-naphthylacetic acid (NAA), the carboxymethyl group is linked to a naphthalene moiety, in case, of 4-HPA it is a phenol which is attached to the carboxymethyl group. Thus, the two compounds differ in a benzene ring instead of a hydroxyl group (Figure 1b,c), leading to the question, whether 4-HPA might mimic auxin-related responses. In case of the natural phenyl-derived auxin phenylacetic acid (PAA), the structural similarity to 4-HPA is even more striking, since it only lacks the hydroxyl group compared with 4-HPA.

This structural similarity is also reflected in the inducibility pattern for auxin-responsive genes by different auxins like indole-3-acetic acid (IAA), or the already mentioned NAA and PAA. To date, NAA and PAA are described to interact with TIR1/AFBs (Sugawara et al., 2015; Tan et al., 2007), and PAA also regulates Aux/IAA and GH3 genes indicating an overlapping or shared signalling pathway with IAA (Sugawara et al., 2015).

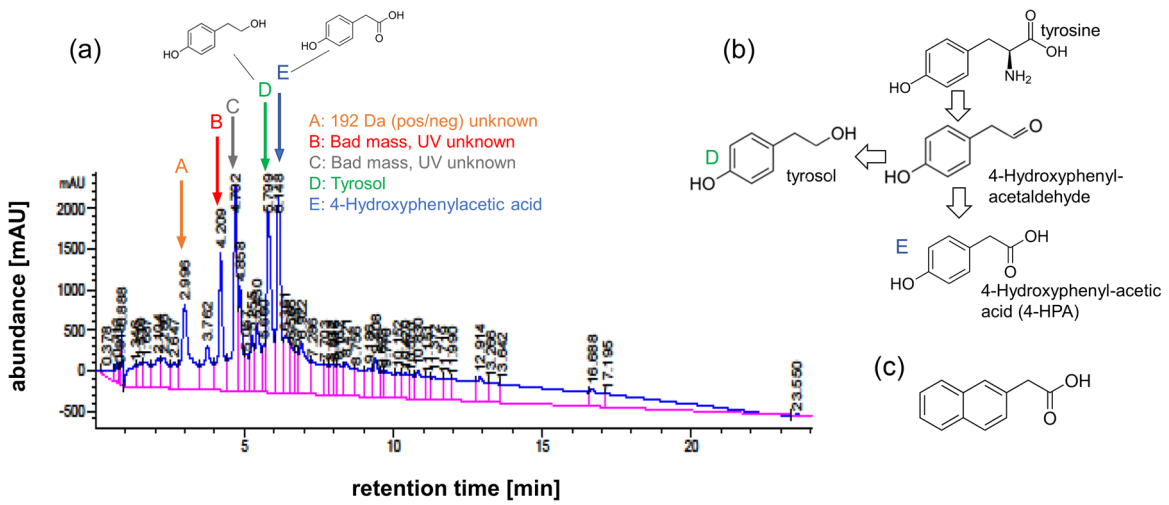

FIGURE 1 Analysis of compounds secreted by *Neofusicoccum parvum* Bt-67 cultivated in the absence of ferulic acid. (a) UV-DAD readouts for an HPLC profile obtained from the hydrophilic phase. For peaks D and E, the shown compounds could be identified by mass spectrometry. (b) Metabolic pathway for the synthesis of the two compounds identified in (a) based on the KEGG database for *N. parvum* (https://www.kegg.jp). (c) Structure of the synthetic auxin 1-naphthalenic acid (NAA). HPLC, high-performance liquid chromatography; KEGG, Kyoto Encyclopedia of Genes and Genomes. [Color figure can be viewed at wileyonlinelibrary.com]

Auxins control various plant responses, mostly related to growth and developmental processes (Naseem et al., 2015). As defence competes with growth for supply of resources, activation of defence is accompanied by a transient reduction in growth rate. The balance between these antagonistic processes is controlled by signals, such as auxins, which activate growth, but inhibit defence to pathogens. For instance, PCD induced by the bacterial elicitor harpin can be mitigated by auxins linked with a suppression of actin bundling in suspension cells of *Vitis* (Chang et al., 2015). The antagonism between auxins and defence is also illustrated by reports, where auxin signalling is downregulated by pathogen-associated molecular pattern recognition in *Arabidopsis*, and, conversely, pathogen susceptibility is silenced after application of exogenous auxins (Navarro et al., 2006). It is not surprising, therefore, that auxins are not only synthesised by plants, but also by plant-associated microorganisms. For instance, another member of *Botryosphaeriaceae* family, *Colletotrichum gloeosporioides*, produces higher levels of auxin (IAA) during its latent phase as compared to the necrotrophic phase, to prolong its lifespan as endophyte inside the host (Maor & Shirasu, 2005).

Since auxins act as negative regulators of plant pathogen defence, the structurally similar 4-HPA might also have regulatory effects on plant defence as to enable the endophytic lifestyle of the fungus. We thus tested the effect of 4-HPA on fungal growth *in planta*, on elicitor-triggered plant cell mortality, as well as on early plant defence responses, such as extracellular alkalinisation, cytoskeletal responses, expression of transcripts linked with auxin-signalling and with defence, as well as metabolites acting as phytoalexins in grapevine, in comparison with the effects of the synthetic auxin NAA. By comparing the effect of 4-HPA with that of NAA a model is proposed where 4-HPA mimics auxin promoting plant growth rather than plant defence.

2 | METHODOLOGY

2.1 | Fungal strains and growth conditions

The fungal strain used in this study was *N. parvum* Bt-67, isolated by the Instituto Superior de Agronomia, Universidade de Lisbona, Portugal (Reis et al., 2016) and kindly provided by the Laboratoire Vigne Biotechnologies et Environement, Université de Haute-Alsace, France. The strain was inoculated from a 30% glycerol stock stored at −80°C by thawing mycelia on ice before cultivation on potato dextrose agar (PDA; Sigma-Aldrich). After incubation in the dark at 28°C for 10 days, mycelia were used for the inoculation into drilled internodes of potted vines.

2.2 | Plant cell lines and their cultivation

To address the cellular and molecular responses, two transgenic *Vitis* suspension cell lines were used. The cell line Vrup-Tub6 derived from *Vitis rupestris*, a wild grapevine from North America, and expresses GFP fused to the N-terminus of ß-tubulin 6 (Guan et al., 2015). The actin-marker cell line Vv-AtFABD2-GFP derived from *V. vinifera* cv. 'Chardonnay' and expresses a fluorescent fimbrin actin-binding domain 2 (AtFABD2), in fusion with a N-terminal GFP (Akaberi et al., 2018). Both cell lines remained under selective pressure of antibiotics and were sub-cultured in weekly intervals into Murashige and Skoog medium and cultivated in darkness at 26°C on an orbital shaker at 150 rpm. All experiments were performed with cells in the expansion phase (4 days post subculture).

2.3 | Preparation of grapevine wood cuttings

V. vinifera cv. 'Müller-Thurgau' were collected during the winter pruning from mature canes of the previous season in 2020. Sections with three buds were rooted in a mixed soil of Peat Moss and Perlite and cultivated in pots for 4 months in the greenhouse at 20°C and 50% humidity during the day and 16°C and 40% humidity during the night, maintaining a day length of 14 h and artificial shading when ambient light exceeded 30 klx.

2.4 | Production and identification of 4-HPA from mycelial liquid culture

Fungal mycelia were pre-cultured for 2 weeks on Potato Dextrose Agar (Sigma-Aldrich). Afterwards, eight plugs (ø 8 mm) of fungal mycelia were picked and cultivated for 2 weeks in Erlenmeyer flasks (500 mL) containing 250 mL of malt extract medium at 20 $g.L^{-1}$ (Carl Roth GmbH), with pH 5.3. The fungal media were separated from the mycelia by 595 Whatman filter paper and a vacuum pump (Schleier & Schüll), and metabolites extracted from the supernatant using an equal volume of ethyl acetate. After evaporation of the organic solvent to dryness under reduced pressure, the crude extract was dissolved in MeOH to a concentration of 20 mg mL^{-1}. We used 20 µL from those concentrates for analysis by high-performance liquid chromatography (HPLC) (Series 1100, Hewlett–Packard; equipped with a LiChrospher RP18 column; 5 µm, 125 × 4 mm, Merck). A gradient of H_2O with 0.1% v/v formic acid and acetonitrile (method: 1% to 100% acetonitrile in 20 min; flow rate: 1 mL min^{-1}) served to fractionate into 96-well plates (Greiner Bio-One, Frickenhausen) and each fraction was analysed then tested for bioactivity (see result section). Further analysis of the fraction led to the detection of one pronounced peak in the hydrophilic phase that was secreted by *N. parvum* exclusively when it had not been challenged by ferulic acid. To identify the active compound in this peak, the crude extract was further re-analysed using an HPLC-MS (Series 1200, Agilent) equipped with an UV-DAD in addition to a coupled LC/MSD Trap APCI-mass spectrometer with positive and negative modes (Buckel et al., 2017). The mass spectrum of this compound (Figure 1) was matching with that of 4-hydroxyphenylacetic acid (4-HPA).

2.5 | *In planta* experiments with 4-HPA and pathogenic fungal hyphae

To address the role of 4-HPA on the fungal development *in planta*, 4-month-old, rooted cuttings (as described above), selected for vigour of foliar and root systems were randomised into four experimental sets: wounded but non-inoculated individuals (mock treatment); wounded individuals that were inoculated in presence of 4-HPA or NAA; wounded individuals infected with *N. parvum* (NP); and wounded individuals pretreated for 1 h with either 4-HPA (HPA+NP) or NAA (NAA+NP) before inoculation with *N. parvum*. For all treatments, inoculation was performed according to Khattab et al. (2021), by drilling into the centre of the stem internode and placing fungal hyphae into the hole before sealing the inoculation site tightly with Parafilm. Pretreated samples were injected into the hole with 200 µL of 50 µM 4-HPA or NAA, respectively, covered and incubated for 1 h before inoculation with the fungal mycelia. After 1 week of incubation, stems were debarked gently, and necrotic areas quantified from digital images as indicated below.

2.6 | Quantification of wood necrosis

The extent of necrotic spread in the infected internode sections was measured as described in Khattab et al. (2021) by quantitative image analysis using the ImageJ freeware (https://imagej.nih.gov/ij). in a predefined section of 7 cm length and 1.5 cm height centred around the wound. The relative necrotic area in percent was calculated by normalisation of the necrotic area to the entire area of the section. Every treatment was represented by at least three biological replications in technical triplicate (scoring three times to account for methodological variability).

2.7 | Quantification of fungal DNA content *in planta*

One week after inoculation, trunk sections (~10–15 mm length and 5–10 mm diameter) were collected, and total genomic DNA was extracted by a slightly modified CTAB method (Doyle J. J. & Doyle J. L., 1987) in 1.5% CTAB buffer and washed with 70% ethanol after precipitation with isopropanol. From this genomic DNA, a *Botryosphaeriaceae*-specific sequence (Ridgway et al., 2011) for the *Internally Transcribed Spacer 1* (*ITS1*) was amplified by genomic PCR under the following conditions: 5 min at 95°C, followed by 35 cycles of 30 s at 94°C, 30 s annealing at 58°C and 1 min elongation at 68°C, followed by a final elongation of 10 min at 68°C. The purified amplicon was used as insert for ligation into the pGEM-T Easy vector (Promega) and transformation of *E. coli* according to the manufacturer protocol. Successful transformants were confirmed by colony PCR before plasmid extraction with the Roti-Prep Mini kit (Carl Roth GmbH) and reconfirmed subsequently by a restriction endonuclease assay and comparison of sequencing data against the NCBI database using BLAST (Altschul et al., 1990). For calibration, C_q values were determined for a 1:10 dilution series from 50 ng to 0.0005 ng plasmid DNA and fitted by linear regression (OriginPro2020 SRI software, OriginLab Corp.), to calculate the absolute amount of fungal DNA in the total genomic DNA extracts.

2.8 | Measurement of extracellular alkalinisation of plant cells challenged with 4-HPA and NAA

Changes in the extracellular pH were followed in Vrup-Tub6-GFP (*V. rupestris*) cells using a pH metre (Schott handylab, pH12), combined with a digital memory recorder, displaying graphic pH readouts at 1-second intervals as an indicator for the steady-state activity of cellular proton pumps as described in Qiao et al. (2010). The suspension cells (4 mL) were pre-adapted on an orbital shaker for 30–60 min before the respective treatment. To address the effect of 4-HPA, and NAA on the activity of proton import, *Vitis* cells were pre-incubated with 50 µM of either 4-HPA or NAA for 30 min before elicitation (9 µg harpin/mL cell suspension). Each measurement was performed in at least 3 biological replicates.

2.9 | RNA extraction and qPCR analysis from challenged plant cells

To address the response of gene expression to 4-HPA and NAA, we used *V. rupestris* (*At*Tub-GFP) cells. All compounds were added after sterile filtration and under sterile conditions into the cell suspension culture before continuing cultivation as described above. Cells were collected after 1 h of the respective treatment, dried using a Whatman filter paper and a vacuum pump (Vacuubrand, Wertheim, Germany), and immediately frozen in liquid nitrogen. Frozen samples were homogenised (TissueLyzer, Qiagen), and total RNA was extracted using an RNA Purification Kit (Roboklon), treated by RNase-free Dnase I (Qiagen) to remove genomic DNA. A template of 1 µg of total RNA was used for cDNA synthesis in the presence of MuLV Reverse Transcriptase, and RNase inhibitor.

The expression of target genes was investigated by quantitative real-time PCR using the CFX PCR System with a C1000 thermal cycler (Bio-Rad) as described in Svyatyna et al. (2014). The C_t values of the respective gene were normalised against *EF-1α* as reference, and the relative steady-state transcript levels were calculated according to Livak and Schmittgen (2001). The details of primer sequences for the target genes are provided in Table S1.

2.10 | UHPLC-MS-based metabolomics of challenged plant cells

To address the potential role of 4-HPA for the regulation of phytoalexin synthesis, we treated *V. rupestris* cells as follows: i) no treatment, ii) 50 µM 4-HPA, iii) 50 µM NAA, iv–vi) the same treatments combined

with 9 µg. mL^{-1} of the cell-death-inducing elicitor harpin. Cellular responses were analysed at three different time points (12, 24, and 48 h), and data were averaged of four biological replications per treatment. The suspended cells were separated from the MS medium (1.5 mL) by a vacuum pump (Vacuubrand), and then the dried cells (100 mg) were directly frozen in liquid nitrogen, before homogenising by a bead mill (TissueLyser II, Qiagen). The *Vitis* metabolites were extracted from the homogenised cells with 100% methanol and analysed by ultra high performance liquid chromatography coupled to mass spectrometry (UHPLC-MS) at INRAE Grand-Est Colmar, France (Duan et al., 2015; Khattab et al., 2021). Here, the chromatographic separation was carried out using a Nucleodur C18 Htec column (150 × 2 mm, 1.8 µm particle size; Macherey-Nagel) as described previously (Martin et al., 2021). The stilbenes were detected by comparing their mass spectra and retention times and compared to those of the corresponding commercial standards. Data were represented in relation to the control readouts of 12 h time point. Differential metabolomic analyses were performed using Tukey's Honest Significant Difference method followed by a false discovery rate (FDR) correction using the Benjamini–Hochberg procedure (Benjamini & Hochberg, 1995). Metabolites of interest were considered differentially accumulated when the false discovery rate was below 5% (FDR < 0.05).

2.11 | Mortality assays with challenged plant cell lines

To probe whether 4-HPA could suppress harpin-dependent cell death, the mortality of *Vitis* cells was quantified using the Evans Blue Dye Exclusion Assay (Gaff & Okong'O-Ogola, 1971). Cells were filtered from MS medium, incubated in 2.5% Evans Blue dye (Sigma Aldrich) for 3–5 min and washed twice with deionised water before microscopic observations. The mortality was determined as the percentage of blue-coloured cells per at least 1000 cells for each replication. Data represent mean values from three biological replicates.

2.12 | Live-cell imaging and quantification of cytoskeletal responses of challenged plant cell lines

Cytoskeletal responses were monitored using the microtubule marker *At*Tub6-GFP which was available in the background of suspension cells from *V. rupestris* (Guan et al., 2015), and the actin marker *At*FABD2-GFP which was available in the background of suspension cells from *V. vinifera* cv. 'Chardonnay' (Guan et al., 2014) by spinning-disc confocal microscopy. Images were recorded as confocal z-stacks as described in Wang & Nick (2017) and processed with the ZEN software (Zeiss). Before observation, the cells were treated with either 50 µM 4-HPA or NAA for 30 min and then observed directly, or, alternatively, treated with 9 µg. mL^{-1} of the cell-death-inducing elicitor harpin for 1 h. Combination treatments were performed by adding 4-HPA or NAA 30 min before harpin and observed after a total incubation time of 1.5 h. The integrity of cortical microtubule bundles and actin filaments was quantified according to Guan et al. (2020) by evaluating grey scale intensity profiles using the ImageJ freeware (https://imagej.nih.gov/ij). For both, microtubules, and actin filaments, 30 individual cells from four independent replicates were scored for each treatment. Statistical analysis was performed as ANOVA Tukey-HSD multiple comparison test with $p < 0.05$ with SPSS Statistics22.0 (IBM Corp.).

2.13 | Growth of the challenged plant cell lines

To assess the effects of 4-HPA and NAA on the growth of each of the suspension *Vitis* cells, Packed Cell Volume (PCV) and sucrose consumption was used as readout (Kaźmierczak et al., 2022). Either 50 µM 4-HPA or NAA were added at subcultivation. The growth index, defined as ratio of PCV at the end of the culture cycle at Day 7 over the initial inoculum at Day 0, was determined from measurements, where 5 mL of cell suspension were transferred into a 15 mL reaction tube and then allowed to sediment overnight at 4°C. Furthermore, the residual sucrose concentration of the culture medium was determined every 24 h for 8 days by refractometry (HI96801, Hanna instruments) beginning at Day 0 directly before the treatment. Data represent mean ± SE from three biological replicates.

2.14 | Statistics

If not stated otherwise, data represent means and SE from three independent biological experiments. Statistical differences were tested by the Tukey LSD test, details are given in the figure legends.

3 | RESULTS

3.1 | *N. parvum* secretes 4-HPA in vitro if not challenged by ferulic acid

During our previous work (Khattab et al., 2022), we had observed that *N. parvum* secretes compounds inducing PCD. This activity was strongly enhanced, when the fungus was confronted with the plant metabolite ferulic acid, the first committed precursor of plant monolignol synthesis. The PCD-responsible molecule could then be identified as Fusicoccin A (FCA). To differentiate ferulic-acid-induced compounds, parallel experiments were conducted, where the fungus was cultivated without ferulic acid (control conditions). Interestingly, under such control conditions using an HPLC-MS strategy, we observed other pronounced peaks in the hydrophilic phase (Figure 1a) that were absent when the fungus was triggered by ferulic acid to secrete FCA. This stimulated the question, how these peaks could be related to the absence of PCD once plant cells are treated with the supernatant collected from the control conditions (without ferulic acid). Among the five peaks found under these control conditions, the first three peaks, with retention times

2.996 min, 4.209 min and 4.702 min, respectively, did not deliver valid mass spectra to be identified (Figure 1a). However, the peak at 5.799 min was identified as tyrosol, and the peak at 6.148 min as 4-HPA. Both compounds are known to be secreted by members of the *Botryosphaeriaceae* family (Masi et al., 2021; Reveglia et al., 2019) and are concurrent derivatives from 4-hydroxyphenylacetaldehyde, a compound generated from tyrosine (Figure 1b). While tyrosol originates from reduction of 4-hydroxyphenylacetaldehyde, 4-HPA is generated by oxidation. The molecular structure of 4-HPA resembles that of the synthetic auxin, 1-naphthaleneacetic acid (NAA). The two compounds differ only by a benzene ring in NAA (Figure 1c) instead of the 4-(hydroxyl group) in case of 4-HPA, leading to the question, whether the fungal 4-HPA, like NAA and natural auxins, might induce responses that are beneficial to plant growth and enable mutualistic interactions during the endophytic phase of this hemibiotrophic fungus.

3.2 | Development of *N. parvum* is promoted by 4-HPA *in planta*

To investigate the role of 4-HPA on fungal development *in planta*, the wood colonisation by *N. parvum* was assessed in plants of *V. vinifera* cv. 'Müller-Thurgau' 3.5 months after initiating cane rooting. The experiment was conducted by pre-treating with either 50 µM 4-HPA or 50 µM NAA for 1 h before the inoculation with *N. parvum*, while a third group was inoculated without pretreatment. The infected internodes were cut, the bark was carefully removed, and the section was imaged digitally at 7 dpi (Figure 2a). The extent of infection was determined by quantitative image analysis as the proportion of wood necrotic area to total trunk area (Figure 2b). To assess the spread of *N. parvum*, the inoculation site of the trunks was sampled in biological triplicates and the abundance of fungal DNA was quantified by qPCR based on a fitted calibration curve (Figure 2c,d).

Only minor necrotic areas in direct proximity of the wound were detectable in mock-treated plants, confirming that wounding itself does not cause extensive wood necrosis. In contrast, infected plants exhibited conspicuously more necrotic areas up to around 33% of the total median area of the trunk (Figure 2b). Although not crossing the threshold for statistical significance, necrosis in infected plants was stimulated by pretreatment with 50 µM 4-HPA (46%) and 50 µM NAA (43%). When we scored the abundance of fungal DNA in infected vines (Figure 2d), we found a parallel pattern for 4-HPA, namely fungal proliferation was increased by 37% over the value seen for inoculation with *N. parvum* alone. In contrast to necrosis, this difference was highly significant. Interestingly, NAA produced a deviating pattern, since it significantly decreased fungal DNA content

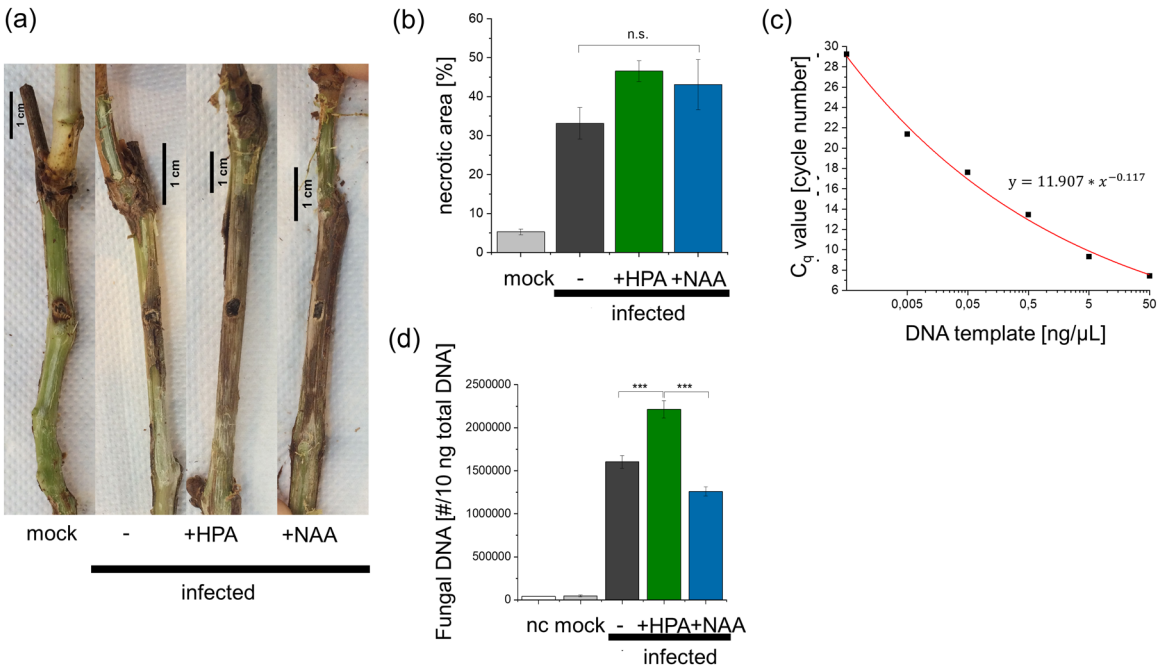

FIGURE 2 Effect of 4-hydroxyphenylacetic acid (4-HPA) or naphthalene acetic acid (NAA) on the interaction between Müller-Thurgau and *Neofusicoccum parvum* (NP). (a) Exemplary images of infected internodes. (b) Necrosis at 7 days post infection (dpi) as percentage of total area of a longitudinal section through the infected internode. (c) Calibration for quantitative PCR using Botryosphaeriaceae ITS primers, black dots are measured values, the red curve is fitted based on an exponential function. (d) Abundance of *N. parvum* DNA at the infection site at 7 dpi. +HPA pretreatment with 50 µM of 4-HPA for 1 h before inoculation, +NAA pretreatment with 50 µM of NAA for 1 h before inoculation. A negative control (nc) was conducted without fungal DNA template to probe for potential cross-contamination of the mock control by other Botryosphaeriaceae fungi not originating from the inoculation. Data represent means and SE from three independent biological experiments. Asterisks indicate statistical differences by the Tukey-LSD test at a significance level with $*p < 0.05$, $**p < 0.01$, $***p < 0.001$. n.s., not significant; SE, standard error. [Color figure can be viewed at wileyonlinelibrary.com]

compared to 4-HPA, and even down to the level seen for inoculation without pretreatment. This was unexpected because necrosis was stimulated by NAA to a similar extent as for 4-HPA. As the fungal DNA content measured for the mock control equalled that of the negative control for the qPCR (nc) negative control (where no fungal DNA template was provided), potential cross-contamination with other innate *Botryosphaeriaceae* species not originating from the inoculation can be ruled out. Taken together, the quantification of fungal copies suggests that treatment with 4-HPA, 1 h before inoculation with *N. parvum*, facilitates the success of fungal colonisation and spread in the host as early as 7 dpi, albeit this is not reflected by any significant increase of necrosis over that seen for the fungus alone. Thus, necrosis cannot be equalled to fungal spread. This was especially evident for NAA that did not significantly promote necrosis but inhibited fungal proliferation.

3.3 | 4-HPA mimics NAA in inhibiting cellular defence responses triggered by harpin

Since 4-HPA promoted fungal spread, we wondered, whether it might quell cellular defence responses as auxins do (Chang et al., 2015). One of the first defence responses is a rapid extracellular alkalinisation, resulting from co-import of protons with calcium ions. This response is mitigated by auxins. Therefore, Vrup-Tub6 cells were pretreated with 50 µM of either 4-HPA or NAA for 30 min before triggering defence with the bacterial elicitor harpin. Harpin alone caused a robust, rapid, and stable extracellular alkalinisation reaching 0.9 units within 30 min, indicative of calcium import (Figure 3a). However, NAA pretreatment reduced this pH response drastically. Interestingly, also 4-HPA pretreatment decreased harpin-triggered alkalinisation in a similar manner by around 50% (Figure 3a).

Since harpin triggers programmed cell death (PCD) in *V. rupestris*, and its deathly effect could be mitigated by auxins (Chang et al., 2015), we tested whether also 4-HPA would behave as an auxin in this regard. Cell mortality was measured using Evans-Blue Dye Exclusion Assay and reached around 45% within 24 h of harpin treatment (Figure 3b). Neither 4-HPA nor NAA induced any mortality beyond the control treatment. However, a pretreatment with these compounds reduced harpin-induced PCD significantly to less than 30%. Similar to harpin, FCA triggers PCD (Khattab et al., 2022). The same experiment performed with FCA (Figure S1) also showed that FCA alone yielded a mortality of 30% within 6 h, while a pretreatment with either 4-HPA or NAA decreased the mortality to a level that was not significantly elevated over the control (Figure S1). Obviously, 4-HPA is able to mitigate PCD.

To get insight into the regulation of defence-related genes by 4-HPA and NAA, the steady-state transcript levels of the phytoalexin synthesis genes, *Phenylalanine Ammonia Lyase* (*PAL*), and *Stilbene Synthases* (*STS16*, *STS27*, and *STS47*), representing different clades of the *STS* gene family, along with the jasmonate responsive *JAZ1* as marker for basal immunity (Chang et al., 2017) were measured (Figure 3c). In response to harpin, the expression of *JAZ1* was mildly elevated. However, harpin strongly boosted transcript levels for all tested phytoalexin biosynthesis genes (*PAL*, *STS16*, *STS27*, and *STS47*). In the absence of harpin, 4-HPA alone did not induce any obvious changes in transcript levels. In contrast, NAA significantly decreased the transcripts levels of *JAZ1*, *PAL*, and *STS16*, but induced the other *Stilbene Synthase* family members (*STS27* and *STS47*). Pretreatment with 4-HPA before elicitation by harpin did not alter the transcriptional responses to harpin with one exception: the induction of *STS27* was eliminated by 4-HPA. This was not seen for pretreatment with NAA. However, NAA produced a mild down-modulation of *STS16* instead. Thus, the effect of 4-HPA (as well as of NAA) clearly differs from harpin-induced extracellular pH and cell

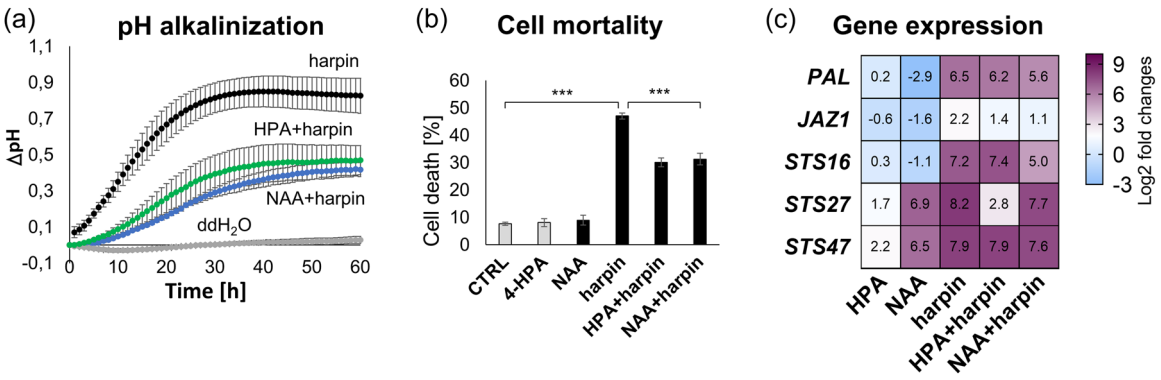

FIGURE 3 4-Hydroxyphenylacetic acid manipulates the steady-state responses of *Vitis* Vrup-Tub6 cells towards harpin. (a) The effect of 4-hydroxyphenylacetic acid (4-HPA) and naphthalene acetic acid (NAA) on the extracellular alkalinization triggered by harpin. Data represents the mean of three independent replicates. (b) The mortality rates in Vitis cells driven by 24 h of harpin alone or in presence of 4-HPA or NAA. (c) Manipulation of steady-state transcripts of stress marker genes in response to harpin alone, combined with 4-HPA, or with NAA. Colour code represents the $\log_2$ fold changes of three biological replicates normalised to the control of the respective time-point. Asterisks indicate statistical differences by the Tukey-LSD test at significance level with $^{*}p < 0.05$, $^{**}p < 0.01$, and $^{***}p < 0.001$. [Color figure can be viewed at wileyonlinelibrary.com]

mortality since 4-HPA partially repressed the accumulation of phytoalexin-synthesis transcripts and showed mitigating effect on pH (as proxy for calcium influx). While both, 4-HPA and NAA, mitigate the response of calcium influx and harpin, they do not modulate the responses of the tested defence-related transcripts in the same manner. There are two striking differences: 4-HPA repressed the harpin induction of *STS27*, while NAA repressed the induction of *STS16* by harpin.

3.4 | 4-HPA suppresses cytoskeletal responses to the bacterial cell death elicitor harpin in plant cells

Cytoskeletons remodelling was studied in response to the bacterial elicitor harpin, using GFP-tagged marker cell lines of grapevine. To follow microtubule responses, a strain expressing *At*TuB6-GFP was available in the background of *V. rupestris*, in the following termed as Vrup-Tub6 (Figure 4). To visualise actin filaments, the marker *At*FABD2-GFP was employed, which was available in the background of *V. vinifera* cv. 'Chardonnay' (Figure 5). Microtubule integrity did not display any obvious difference after 30 min of treatment with either 4-HPA (Figure 4b) or NAA (Figure 4c), compared to the control (Figure 4a). On the other hand, cortical microtubules were strongly disrupted and depleted, when assayed 60 min after harpin treatment (compare Figure 4a–d). This disruption of cortical microtubules was mitigated by pretreatment with 4-HPA (compare Figure 4d,e), and, likewise, by pretreatment with NAA (compare Figure 4d,f). A quantification of microtubule integrity (Figure 4g) showed that harpin alone caused a significant ($p < 0.05$) reduction of microtubule integrity, while there was no significant difference between control and cells pretreated with 4-HPA and NAA before being challenged with harpin.

We also assessed the response of actin filaments known to be often involved in PCD. In the control, actin was pre-dominantly organised in a cortical network of fine filaments (Figure 5a). Again, actin network did not exhibit any obvious changes after 30 min of pretreatment with 4-HPA or NAA (Figure 5b,c). In contrast, after 60 min of harpin treatment, the cortical actin network was eliminated completely. Instead, transvacuolar actin cables emerged, accompanied by short actin rods, indicative of perturbed integrity (compare Figure 5d and the control Figure 5a). As for microtubules, pretreatment with 4-HPA and NAA effectively alleviated this response of actin filaments to harpin and fully restored the cortical network (compare Figure 5a,d–f). Again, a quantification of actin integrity

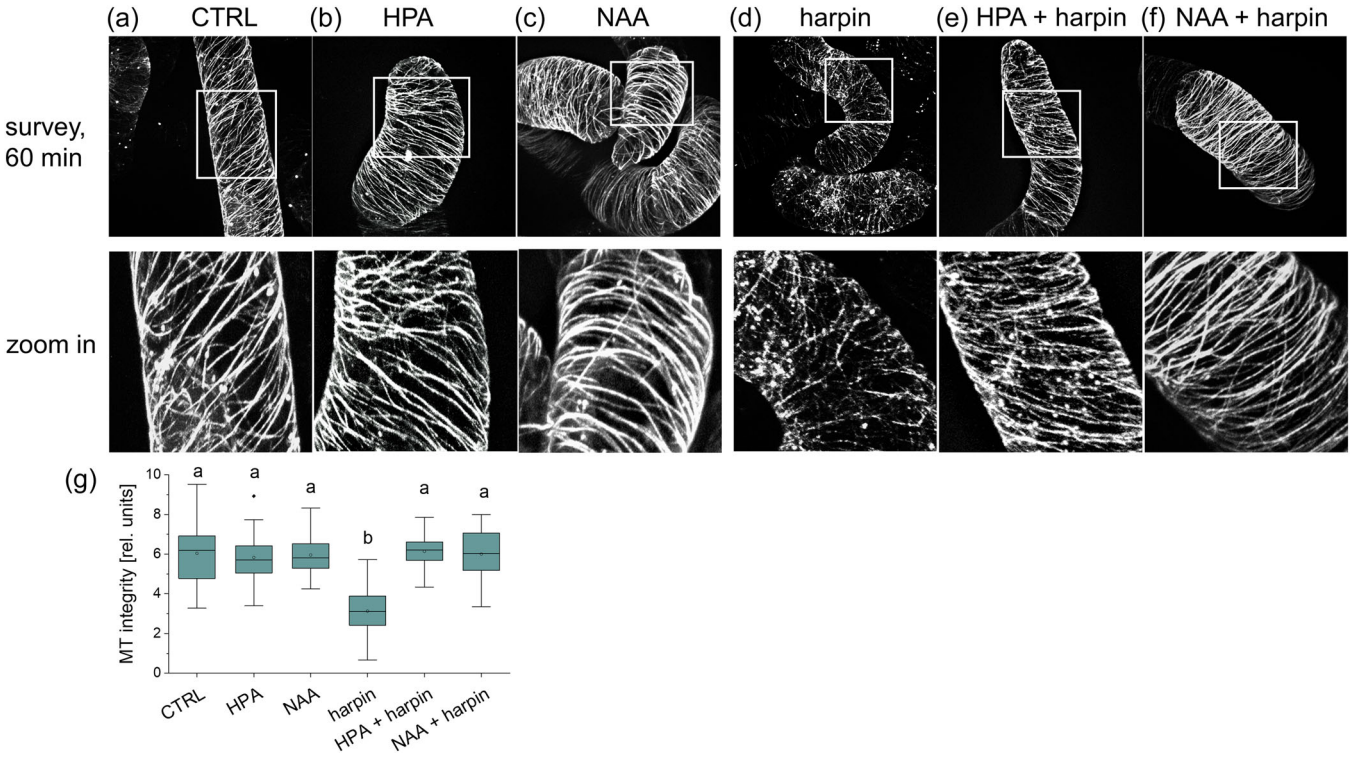

FIGURE 4 Effect of pretreatment with either 50 µM 4-hydroxyphenylacetic acid (4-HPA) or naphthalene acetic acid (NAA) for 30 min on the microtubular response to the bacterial cell death elicitor harpin, followed by live-imaging of Vrup-Tub6-GFP cells (*V. rupestris*). Representative cells are shown either for treatment without (a–c) or with subsequent harpin (9 µg/ml) treatment for 60 min (d–f). Not pretreated cells are shown in (a, d), pre-treatments with 50 µM 4-HPA for 30 min in (b, e), pre-treatments with 50 µM NAA for 30 min in (c, f). (g) Quantification of microtubular integrity for the treatments shown representatively in (a–f). Data represent medians, interquartiles, and extreme values for measurements from 30 individual Vrup-Tub6 microtubule-marker cells. Different letters represent statistical differences based on the Tukey-HSD test with significant levels $p < 0.05$ in (g). [Color figure can be viewed at wileyonlinelibrary.com]

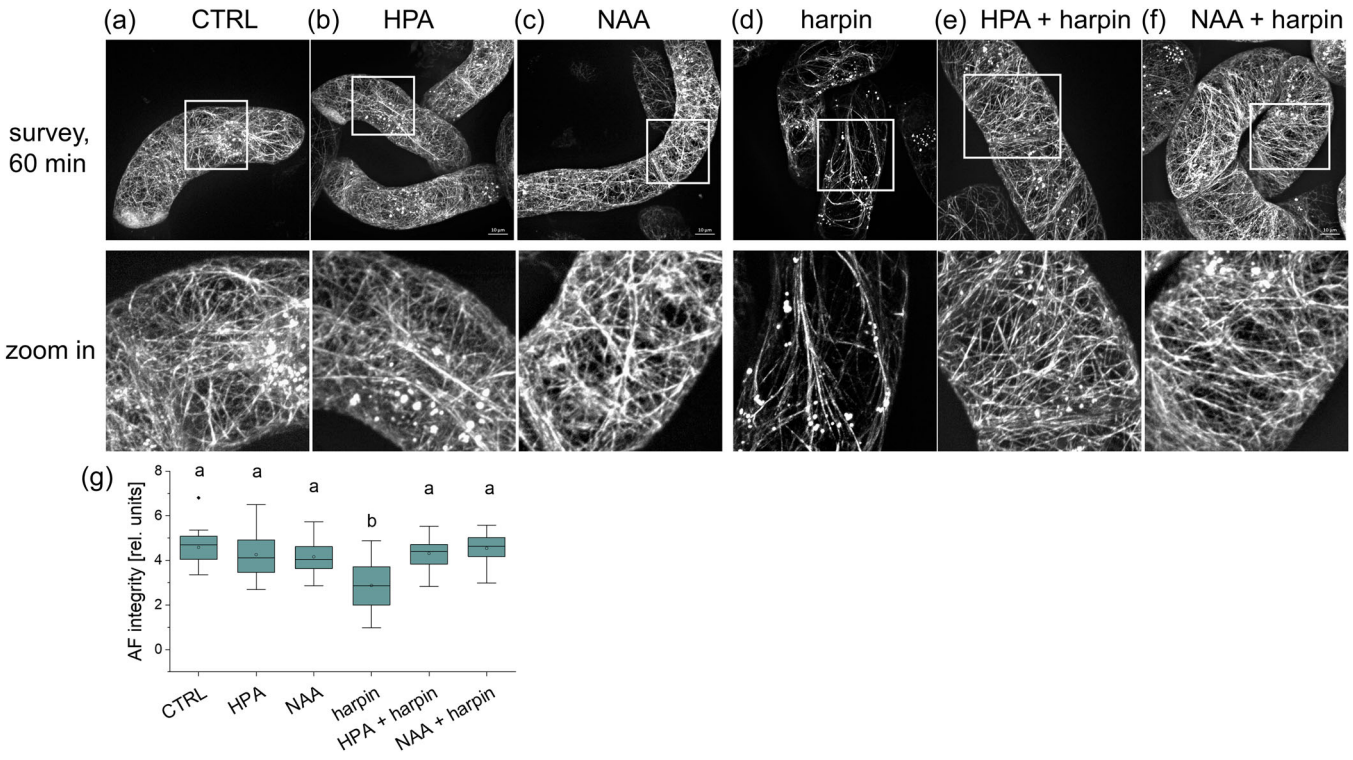

FIGURE 5 Effect of pretreatment with either 50 µM 4-hydroxyphenylacetic acid (4-HPA) or naphthalene acetic acid (NAA) for 30 min on the actin filament response to the bacterial cell death elicitor harpin, followed by live-imaging of Vv-*At*FABD2-GFP cells (*V. vinifera*). Representative cells are shown either for treatment without (a–c), or with subsequent harpin (9 µg/mL) treatment for 60 min (d–f). Not pretreated cells are shown in (a, d), pre-treatments with 50 µM 4-HPA for 30 min in (b, e), pre-treatments with 50 µM NAA for 30 min in (c, f). (g) Quantification of actin network integrity for the treatments shown representatively in (a–f). Data represent medians, interquartiles, and extreme values for measurements from 30 individual Vv-*At*FABD2-GFP actin-marker cells. Different letters represent statistical differences based on the Tukey-HSD test with significant levels $p < 0.05$ in (g). [Color figure can be viewed at wileyonlinelibrary.com]

(Figure 5g) confirmed a significant drop ($p < 0.05$) for harpin treatment, while there was no significant difference with the control for all other treatments. Thus, 4-HPA and NAA can suppress the cytoskeletal changes induced by harpin when trigging cell-death related defence.

3.5 | 4-HPA and NAA modulate the accumulation of stilbenes in response to harpin

Since 4-HPA and NAA could inhibit the earlier defence responses triggered by harpin both at the molecular and cellular level (Figures 3–5), we try to decipher how this would modulate metabolic responses. We, therefore, followed thirty-four metabolites (including amino acids, phytohormones and phytoalexins) over time in Vrup-Tub6 cells (Figure S2). Based on the peak areas, amino acids were the most dominant metabolites, especially phenylalanine, followed by glutamine. Also, valine and leucine/iso-leucine were relatively abundant. However, none of these most abundant amino acids displayed any significant fluctuation over time or in response to harpin, nor to 4-HPA and NAA (Figure S1). The same holds true for the majority of the other, less-abundant amino acids. A few exceptions were noted, though. Mainly cysteine, but also glutamic acid, responded, albeit in different patterns. For the jasmonate pathway, the precursor OPDA was far more abundant than its derivatives JA and MeJA but remained fairly constant for all of the tested conditions. Also, the cytokinin zeatin was constitutively detected in levels similar to those of OPDA, but with no changes. Salicylic acid was low as well, with some weak changes. Among the antioxidants, ascorbate was not changing, while glutathione, which was very abundant, did. These changes paralleled those of the glutathione precursor, cysteine. The stilbenes were the metabolites with the lowest ground levels, but also the metabolites with the most pronounced change. The strongest induction was observed for the combination of harpin with NAA, which was also the condition, where glutamate, cysteine and glutathione were most elevated.

A principal component analysis (PCA) performed on all quantified metabolites indicated that the metabolic profiles of NAA-Harpin-treated cells were significantly different from the profiles under the other experimental conditions at all tested time points (Figure 6a). To compare the profile of a particular metabolite among treatments and time points, the readouts were normalised to the value found in control cells of 12 h-time point (Figure 6b).

There were no remarkable changes in amino acids profiles if the metabolites were visualised together with the phytoalexins. However, when both groups of metabolites were scrutinised separately,

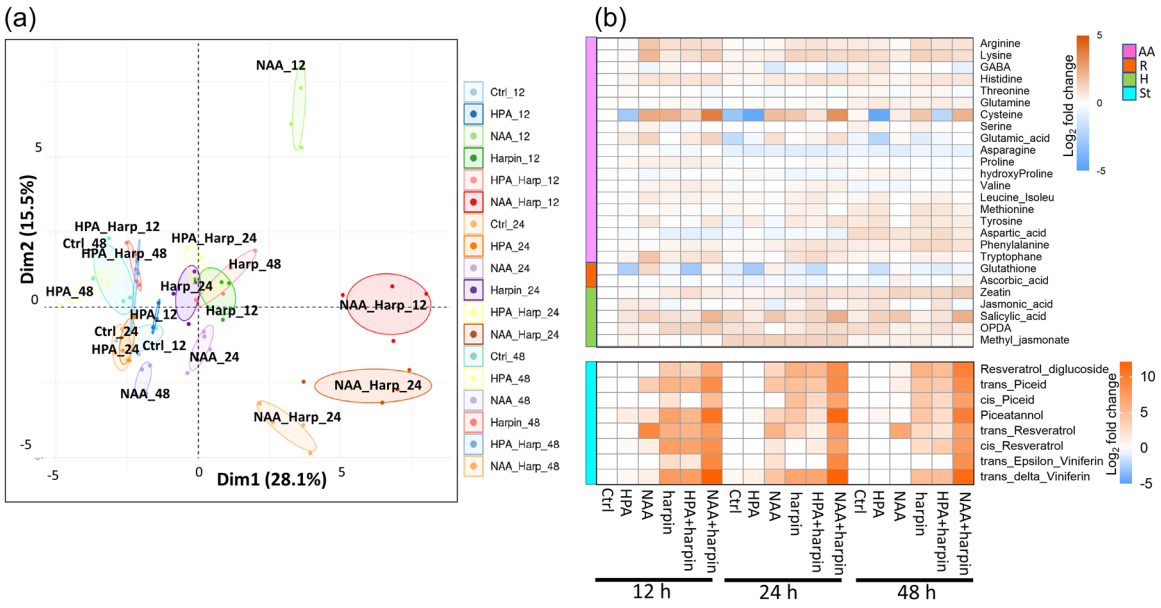

FIGURE 6 Metabolic impact of combined 4-hydroxyphenylacetic acid (4-HPA), naphthalene acetic acid (NAA) and harpin treatments on Vrup-Tub6 cells. (a) Principal component analysis (PCA) of the metabolomic data sets. The first and the second principal components explained 28% and 15.5% of the variance separating the groups of samples, respectively. (b) Heat map of metabolic changes in Vrup-Tub6 cells treated with 4-HPA or NAA or combined with the bacterial elicitor harpin. Indicated metabolites were quantified at three time points (12, 24, and 48 h) posttreatment in the following samples: control (Ctrl), 4-HPA-treated cells (HPA), NAA-treated cells (NAA), Harpin-treated cells (Harpin), cells treated with both 4-HPA and Harpin (HPA+Harp), and cells treated with both NAA and Harpin (NAA+Harp). Readouts were normalised to the value of control cells at 12-h-time point. Log_2 ratios of fold changes from control cells at 12 h (Ctrl, 12 h) are given by shades of red or blue colours according to the scale bar. The metabolites were grouped as amino acids (AA), hormones (H), reducing agents (R) and stilbenes (St). Data represent mean values of four biological replicates per each treatment and time point. [Color figure can be viewed at wileyonlinelibrary.com]

adjusting the scale, some responses of cysteine could be discerned (Figure 6b). While harpin and NAA induced cysteine accumulation and apparently interacted additively, 4-HPA decreased the accumulation of cysteine, no matter, if given alone or in combination with harpin. This pattern was mirrored by parallel changes (albeit at much lower amplitude) of the cysteine derivative glutathione. However, the most prominent changes were observed for phytoalexin synthesis. The first committed metabolite of the stilbene pathway, *trans*-resveratrol, was significantly (by more than an order of magnitude) induced by NAA, to a lesser extent by harpin. Combining NAA and harpin yielded more than harpin alone, but less than NAA alone. In contrast, combining 4-HPA and harpin decreased the trans-resveratrol content at 24 h, as compared to harpin alone. For the isomer, *cis*-resveratrol, the pattern was different because NAA alone caused mild increase, but enhanced the harpin response. The *trans*-resveratrol glucoside *trans*-piceid was induced by both, harpin and NAA, with an additive effect of their combination. For none of these stilbene monomers did 4-HPA show any effect. Interestingly, the induction of the *cis*-resveratrol glucoside, *cis*-piceid, was quelled by 4-HPA, while NAA was enhancing the effect of harpin. For the stilbene oligomers *trans*-δ-viniferin and *trans*-ε-viniferin, the synergy between NAA and harpin was very pronounced, because, here, NAA did not produce any remarkable effect, while it strongly increased the amplitude of the response to harpin. However, again, 4-HPA was ineffective, no matter, whether given alone or together with harpin. In contrast, for the hydroxylated resveratrol derivative piceatannol as well as for resveratrol-diglucoside, the effect of NAA was adding up to that of harpin, while 4-HPA dampened the induction by harpin, while not yielding any effect, if given alone.

Thus, although NAA and 4-HPA showed similar effects on the extracellular alkalinisation and cellular responses, such as mortality or cytoskeletal integrity, the two compounds acted differently with regard to the induction of stilbene compounds.

To pinpoint the effects of 4-HPA on the stilbene pathway, we calculated the ratios for the effects of 4-HPA over the control, that of harpin over the control, and that of the combination of 4-HPA and harpin over harpin alone (Figure 7).

Harpin alone upregulated the synthesis of all tested stilbenes, albeit with different time courses. *Trans*-resveratrol accumulated rapidly with a peak at 12 h and gradually decreased subsequently. Its glucoside, *trans*-piceid, was strongly induced from the first measured time point (12 h), but persisted thereafter, as did its derivative resveratrol-diglucoside. In contrast, *cis*-resveratrol accumulated as swiftly as *trans*-piceid but dissipated much more swiftly as well. The respective glucoside, *cis*-piceid was the only tested metabolite that accumulated with a delay (actually concomitantly with the disappearance of *cis*-resveratrol). A similar time-course was seen for δ-viniferin, but it persisted over the entire 48 h of the experiment (contrasting with *trans*-ε-viniferin which was observed only at 12 h). Likewise, the hydroxylated piceatannol was induced rapidly, and remained

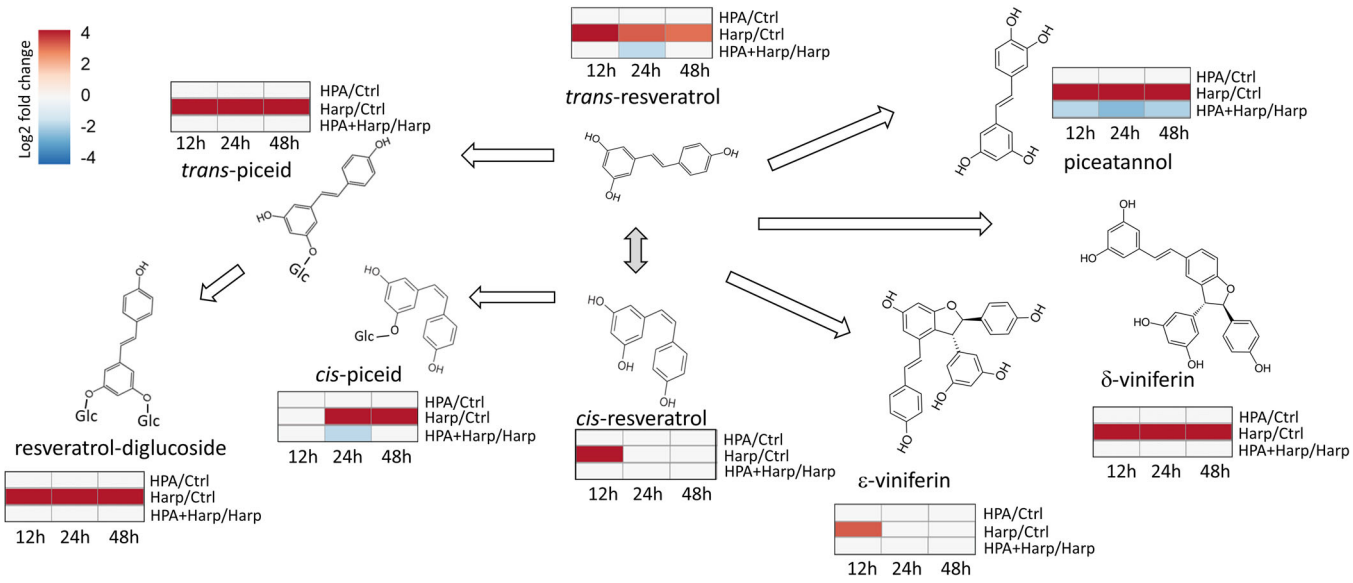

FIGURE 7 The fungal polyketide 4-Hydroxyphenylacetic acid (4-HPA) partially inhibits harpin-induced stilbene accumulation. Log_2 of significant metabolite fold changes are given by shades of red or blue colours according to the scale bar, for the following pairwise comparisons at three time points (12, 24, and 48 h): 4-HPA-treated cells as compared to control cells (HPA/Ctrl); harpin-treated cells as compared with control cells (Harp/Ctrl); and cells treated with both 4-HPA and Harpin as compared to Harpin alone (HPA+Harpin/Harpin). Readouts were normalised to the value of control cells at 12-h-time point. Data represent mean values of four biological replicates for each condition and time point. Statistical analyses were performed after Log_{10} transformation, using the Tukey's Honest Significant Difference method followed by a false discovery rate (FDR) correction, with FDR < 0.05. For FDR ≥ 0.05, Log_2 fold changes were set to 0. [Color figure can be viewed at wileyonlinelibrary.com]

elevated. Overall, the pretreatment of 4-HPA had very little effect on the metabolic response to harpin, illustrated by the fact that the ratios of the abundance for the combinatorial treatment over harpin alone were close to 1 throughout. However, there are three exceptions: 4-HPA significantly reduced the accumulation of *trans*-resveratrol, *cis*-piceid, and piceatannol in harpin-treated cells, especially at 24 h (Figure 7).

In summary, both, 4-HPA and NAA, modulate the cytological responses to harpin in a similar manner, namely, they quell mortality and cytoskeletal remodelling. However, the two compounds differ regarding the regulation of stilbene accumulation. Here, while NAA strongly induced the synthesis of the resveratrol derivatives, ε-viniferin and piceatannol, in presence of harpin (Figure 6), 4-HPA repressed the effect of harpin on the regulation of *STS27* (Figure 3c) and prevented the accumulation of trans-resveratrol and its derivatives piceatannol and *cis*-piceid (Figure 7).

3.6 | 4-HPA mimics auxins in grapevine cells, but only with respect to defence

To distinguish whether 4-HPA, due to its structural similarity with phenylacetic acid (PAA), might exert auxin-like activities, we investigated induction of genes linked with auxin-signalling, inactivation, and response, along with the effect on cell culture growth (Figure 8). We measured the steady-state transcript levels for the auxin-response gene *AUX/IAA4*, reported to be transiently induced by NAA in young grapevine leaves (Çakir et al., 2012), for the cognate transcription factor *Auxin Response Factor 1* (*ARF1*), as well as for the auxin-responsive auxin-amino acid conjugate *Gretchen Hagen 3* (*GH3*). These measurements were made 60 min after adding 50 μM of either NAA, 4-HPA, or indole acetic acid (IAA), respectively (Figure 8a). While the expression patterns for *AUX/IAA4* and *ARF1*, were similar for IAA and 4-HPA, *GH3* transcripts clearly differed. The *GH3* transcript levels were induced by IAA, with this respect resembling *AUX/IAA4* and *ARF1*. However, only *GH3* was repressed in response to 4-HPA. Hereby, IAA was more efficient in inducing *ARF1*, while 4-HPA was more efficient in triggering *AUX/IAA4*. Interestingly, NAA did not cause a strong induction in any of the three transcripts. Thus, 4-HPA induced expression of transcripts involved in auxin signalling and repressed expression of a transcript involved in auxin conjugation.

The growth index of the cell suspension culture was determined as the sedimented cell volume to total volume ratio of day 7 over day 0 (Figure 8b). 4-HPA did not significantly alter culture growth in comparison to the control, whereas the growth index of cells treated with NAA was significantly smaller. This was also reflected by the consumption of sugar as readout for cell expansion (Figure 8c), which was significantly weaker in cells treated with NAA, indicating a slower development by NAA (Figure 8c). In the contrary, sucrose content decreased significantly stronger in response to 4-HPA, suggesting a stimulation of cell expansion. Thus, the effect of the three auxins on cell expansion runs in parallel with their effect on the expression of *Aux/IAA* and *ARF1* transcript levels. While NAA is not inducive,

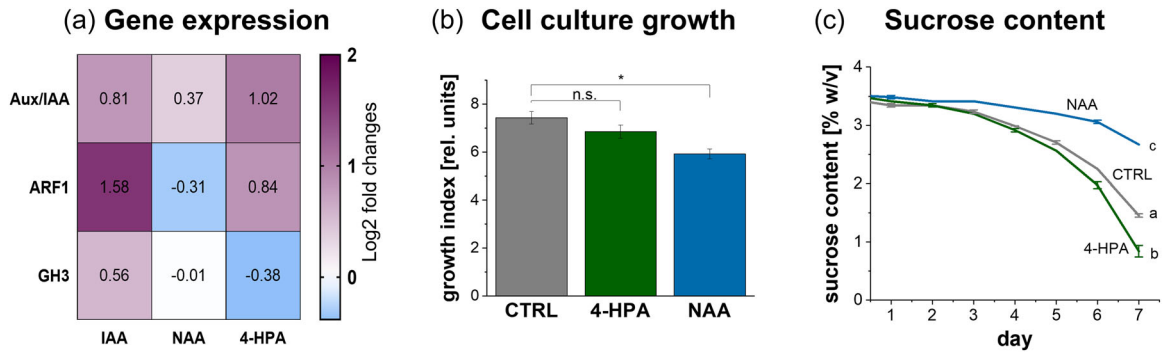

FIGURE 8 4-Hydroxyphenylacidic acid (4-HPA) induces auxin-responsive genes but does not inhibit cell culture growth in Vrup-Tub6 cells. (a) Induction of steady-state transcripts of Auxin-responsive genes by naphthalene acetic acid (NAA), indole-3-acetic acid (IAA) and 4-HPA as $\log_2$ fold change to the untreated control. (b) Growth index as cell volume to total volume ratio of Day 7 over Day 0 treated with NAA or 4-HPA. Asterisks indicate statistical differences by Tukey-HSD test at significance level $\alpha < 0.05$ with $^*p < 0.05$. (c) Change of sucrose content in cell suspension culture medium following treatments with NAA or 4-HPA. Statistically homogenous subsets at Day 7 by Tukey-HSD are indicated by subset letters at significance level $\alpha < 0.05$. Data represents three biological replicates normalised to the control of the respective time-point. [Color figure can be viewed at wileyonlinelibrary.com]

neither for auxin signalling, nor for auxin conjugation, 4-HPA is inducing for auxin signalling, but not for auxin conjugation, which is in good correlation with stimulated cell expansion.

4 | DISCUSSION

Botryosphaeriaceae-dieback (BD) is a conditional disease, where the associated fungi colonise the host as endophytes over the years, but then can turn pathogenic and trigger an apoplectic dieback (sometimes also a slow dieback), often during a hot and dry summer. Guided by the working hypothesis that the interaction of host and pathogen is controlled by chemical signals, we identified, using the aggressive strain *Neofusicoccum parvum Bt-67* as a model, the plant monolignol precursor ferulic acid as "surrender signal" triggering the fungus to release PCD-inducing FCA (Khattab et al., 2022). While FCA plays a role in initiating the fungal necrotrophic phase, we hypothesised that alternative fungal signals might act during the endophytic phase and downregulate plant immunity for fungal colonisation. Such signals are expected to be secreted in the absence of ferulic acid. The fungal metabolite 4-hydroxyphenylacetic acid (4-HPA) was identified as candidate meeting this criterion in vitro. Due to its structural similarity with naturally occurring auxins, we also explored the possibility that 4-HPA partially deploys auxin signalling to support plant colonisation by *N. parvum* during the endophytic phase before switching to necrotrophy. Using an infection assay *in planta*, we finally assessed the molecular and cellular aspects of plant cell defence when challenged with 4-HPA compared to auxin molecules. In the following, we discuss, to what extent 4-HPA can be considered as auxin mimic, whether its effect on defence-related cytoskeletal remodelling might be functionally linked to this auxin activity, whether the effect of 4-HPA is specific, and what role 4-HPA might play for the successful colonisation of the host.

4.1 | Does 4-HPA mimic auxin?

4-HPA is a hydroxylated derivative of phenylacetic acid (PAA), a natural auxin discovered in a wide variety of plant species more than forty years ago (Wightman & Lighty, 1982). The synthesis of PAA is discussed controversially. While enzymes from the *TAA1* and *YUCCA* gene families that are responsible for the conversion of tryptophan into indole-3-pyruvic acid and then towards IAA, were suggested to be involved (Sugawara et al., 2015), there is meanwhile strong evidence indicated that PAA does not share the same precursor as IAA. Indeed, while IAA is mostly generated from tryptophane, PAA is created via phenylpyruvate from phenylalanine (Cook & Ross, 2016; Cook & Nichols, Smith, et al., 2016). Nevertheless, as a derivative of PAA, 4-HPA might act as auxin. In fact, this is partially the case for our grapevine suspension cells.

With respect to defence responses, 4-HPA behaves as an auxin in most, but not in all aspects. The suppression of extracellular alkalinisation (Figure 3a), PCD (Figure 3b), harpin-induced expression of *STS27* (Figure 3c), as well as of the response to the bacterial elicitor harpin, mimics the effect of auxin on host cell defence (Figure 4). Additionally, 4-HPA resembles the effects of NAA, and are consistent with auxin effects reported for the same cell system earlier (Chang et al., 2015). Interestingly, this similarity between 4-HPA and auxins does not hold, when the stilbene metabolites are considered (Figures 6 and 7).

Auxins are not primarily known as silencers of plant defence, but as activators of plant growth. Cell growth seems to be only poorly mimicked by 4-HPA, although it significantly stimulated sucrose consumption used as proxy for cell expansion (Figure 8c), as well as the activation of early auxin-induced genes. While transcripts of two genes involved in auxin signalling were induced by 4-HPA as they are by IAA, we found that expression of *GH3*, encoding a protein involved in auxin conjugation, was repressed by 4-HPA, while being induced by IAA. Auxin-amido synthetases like GH3 are thought to

play a role in defence, because they not only remove IAA but simultaneously promote the formation of PAA, a pathway giving rise to the highly potent shunt product phenylacetonitrile (Aoi et al., 2020). Thus, the downregulation of *GH3* by 4-HPA is expected to increase IAA activity, while the defence-related activation of the PAA pathway would be suppressed. In other words: 4-HPA might quench defence through three routes. 1. By downmodulating GH3, 4-HPA would shield IAA from inactivation by conjugation, such that IAA would mitigate defence. 2. By downmodulating GH3, 4-HPA would silence the PAA pathway and, thus, prevent the accumulation of the defence compound phenylacetonitrile. 3. By activation of AUX/IAA and ARF1, 4-HPA would activate auxin signalling towards a stimulation of growth.

Summarising, 4-HPA, by its structural similarity with PAA, hijacks auxin signalling, shifting the plant from defence towards growth. This sophisticated manipulation might underly the promoted colonisation in presence of 4-HPA (Figure 2).

4.2 | Modulation of actin responses by 4-HPA might act upstream of 4-HPA mitigated PCD

The auxin responses that are mimicked by 4-HPA comprised also the mitigation of harpin-induced remodelling of both, microtubules (Figure 4) and actin filaments (Figure 5). This 4-HPA effect on the cytoskeletal response might be linked with the mitigated defence-related mortality in response to harpin (Figure 3b), and similarly with the fungal toxin FCA (Figure S1). However, the remodelling of microtubules and actin filaments might also be a parallel phenomenon that is not causally linked with the silencing of PCD by 4-HPA. It seems that the answer must differ for microtubules and actin filaments:

The elimination of microtubules by harpin can be blocked, when microtubules are pre-stabilised by taxol (Guan et al., 2021). The same holds true for the fungal toxin FCA, however, without reducing the mortality induced by FCA (Khattab et al., 2022). Conversely, the effect of harpin on microtubules can be mimicked by oryzalin that by itself, fails to induce a mortality response (Guan et al., 2021). Thus, the microtubule response in response to harpin or FCA and the mortality induced by these compounds seem to be specific for the two molecules and could be parallel phenomena rather than sequential steps of a causal chain.

For the remodelling of actin, the situation looks different. Here, the elimination of actin filaments by Latrunculin B suppresses both, the cell-death response to harpin (Chang et al., 2015), and the mortality triggered by FCA (Khattab et al., 2022). Thus, actin remodelling is necessary for defence-related PCD. This role of actin remodelling is not confined to grapevine cells but represents a general phenomenon (for review see Smertenko and Franklin-Tong, 2011). The remodelling is a complex process where cortical actin is depleted, followed by actin bundling into transvacuolar cables. Several molecular players of this remodelling have been identified, such as actin depolymerisation factors (Tian et al., 2009), capping proteins (Li et al., 2017), or formins (Du et al., 2021). Actin remodelling is triggered by reactive oxygen species (ROS) deriving from the NADPH oxidase Respiratory burst oxidase Homologue (RboH) in the plasma membrane (Chang et al., 2015; Li et al., 2017). However, actin remodelling is not sufficient to induce PCD, because it can be induced by aluminium ions (Wang et al., 2022) as well as by glycyrrhizine (Wang et al., 2021) without leading to a cell death response. On the other hand, 4-HPA can suppress actin remodelling in response to harpin (Figure 5e) which is linked with a reduced mortality response to harpin (Figure 3b), which tells that actin remodelling is necessary to induce PCD.

The effect of 4-HPA on actin and PCD represents a further case, where auxins can suppress actin remodelling (Nick et al., 2009). This seems to be the reason, why defence-related PCD can be mitigated by auxins. The mechanism underlying this auxin effect seems to be the depletion of triggers for actin remodelling, namely ROS, by the recruitment of ROS for auxin signalling (Eggenberger et al., 2017). As a result, auxin-stimulated growth and ROS-induced actin remodelling are competing for a limited pool of ROS near the plasma membrane. Such an "actin-auxin oscillator" model indicates that 4-HPA could be a compound that can mimic auxin with respect to cell expansion (actin remodelling, Figure 5e), while quenching defence-related PCD (Figure 3b). Since a fluorescent actin-marker line is available only for *V. vinifera* cv. 'Chardonnay' and not for *V. rupestris*, which was the model for most of the study, there is the question, whether the two genotypes might differ in their susceptibility to *N. parvum* Bt-67. However, a systematic infection study, where both genotypes were tested along with numerous other varieties of *V. vinifera* and other species of *Vitis* (Guan et al., 2016), showed that both genotypes are highly susceptible, such that actin responses in the two genotypes are most likely comparable.

4.3 | 4-HPA and NAA manipulate phytoalexins synthesis in a different way

While 4-HPA and NAA could modulate some of the defence responses deployed by harpin, such as calcium influx or cytoskeletal remodelling, their effect on stilbene synthase transcripts and stilbene metabolites was relatively subtle and specific (Figures 3c, 6, and 7). These phytoalexins are central antimicrobial molecules to prevent the local development of pathogenic fungi in grapevines, such as the Oomycete *Plasmopara viticola* causing Downy Mildew (Duan et al., 2015), the Ascomycetes *Erysiphe necator* causing Powdery Mildew (Jiao et al., 2016), and *Botrytis cinerea* causing Grey Mold (Adrian and Jeandet, 2012). The key enzyme driving the first committed step of the stilbene pathway, stilbene synthase, is encoded by an unusually large gene family with more than 40 members (Parage et al., 2012). By heterologous transient expression in *Nicotiana benthamiana*, these were found to be endowed with a similar enzymatic activity. Likewise, the sequences, especially those in the active centre, are very similar, speaking against a model, where the individual members drive different enzymatic reactions. If at all,

only one amino-acid exchange located outside of the active centre, has been proposed to mediate interaction with different binding partners. Instead, the rapid radiation of this gene family seems to be linked to differential regulatory patterns (Parage et al., 2012). Considering that the general effect of the two auxins is mild, three salient features should be mentioned: NAA induces the transcripts of *STS27* and *STS47* (but not *STS16*) and triggers the accumulation of *trans*-resveratrol, while 4-HPA caused only mild effects. In combination with harpin, NAA repressed *STS16*, but induced the accumulation of *trans*-resveratrol and its derivative piceatannol, as well as of *trans*-ε-viniferin. In contrast, 4-HPA blocked the induction of *STS27* transcripts by harpin and blocked, transiently, the accumulation of *trans*-resveratrol and its derivatives piceatannol and *cis*-piceid (Figures 3c and 6). Furthermore, 4-HPA caused a mild and transient downmodulation of *trans*-resveratrol.

It is, therefore, possible that the differential effect of the two molecules on fungal spread was linked to their differential effect on *trans*-resveratrol and piceatannol (Figure 6). When the induction of these two compounds in response to a pathogen is blocked by 4-HPA, this is expected to favour fungal spread, while amplification of their induction and accumulation should inhibit fungal spread (NAA effect). In good accordance, *in planta* the abundance of fungal DNA is significantly increased by 4-HPA but significantly decreased by NAA (Figure 2c). Interestingly, the effect on fungal spread is not mirrored by a corresponding effect on the necrotic areas. These were not significantly different from those seen for plants infected by the pathogen alone. Thus, the presence of the fungus does not necessarily mean necrotic death. In other words: in the presence of 4-HPA the fungus can spread better but prevent host necrosis. This is consistent with a model, where 4-HPA acts as a factor sustaining the fungus endophytic and possibly preventing a switch to necrotrophy.

Since most of these observations have been collected in a grapevine cell culture system, the question arises, to what extent these findings can be transferred to the situation in real plants. A comparative study using standardised infection with *N. parvum* in different hosts (Khattab et al., 2021) showed an interesting commonality: the most resilient *sylvestris* genotype, Ke15 differs from the more susceptible genotypes Ke13 and Ke94 by a more vigorous and swifter (2 d), but transient induction of piceatannol, indicating that this compound could be considered as a marker of local and basal resistance *in planta*, enabling fungistatic activity that delay conidia germination and hyphal growth (Hedenström et al., 2016) When 4-HPA quells the induction of this defence marker, this would account for the observed promotion in non-pathogenic fungal spread (Figure 2d). To what extent the accumulation of piceatannol is linked with the induction of *STS27* (the stilbene synthase, i.e., specifically quelled by 4-HPA) remains a rewarding topic for future research. It should be emphasised, though, that stilbene synthases show a certain promiscuity and can accept phenolic substrates other than coumaryl-CoA (Chong et al., 2009). For instance, piceatannol in pine can be produced by a specific stilbene synthase that accepts feruloyl-CoA as substrate (Raiber et al., 1995). Whether grapevine STS27 can act as a piceatannol synthase, is not known, but would be a testable implication of a working model, where 4-HPA specifically targets or controls to this branch of the stilbenoid pathway.

4.4 | What is the function of 4-HPA for *N. parvum*?

Since it had been coined by Antoine de Bary (1866), the term endophyte has experienced a manifold and often contradictive history of use leading to pleas for dropping it altogether (for an insightful review see Wilson, 1995). However, the term is important to discriminate symptomless colonisation from necrotrophy or of biotrophy. It should also be discriminated from the term chronic form of BD, where parts of the plant die off, while other parts are still able to grow. The fungus can still persist in the dead parts and attack the surviving part until this will yield, too (although this process can extend over years, and, thus, differs from apoplectic breakdown). After all, in this chronic progression, the fungus behaves as a necrotroph, not as an endophyte. A carefully conducted evolutionary study (Delaye et al., 2013) has revealed that the transition between endophytic growth and necrotrophy occurs frequently and is reversible at the evolutionary and even ecological timescale, while biotrophy is a one-way road. Mutations that enable an endophytic lifestyle will, thus, not channel subsequent changes – they are not following the pattern of Muller (1964). This is interesting because both, endophytic and necrotrophic lifestyles, modulate the immune response of the host. 4-HPA is certainly not the only factor relevant here and further experiments will be required to specify the determinant value of it maintaining the fungal endophytic lifestyle. During a comparative study, the *N. parvum* strain Bt-67 was found to secrete high levels of (-)-terremutin, but almost no (R)-mellein, diverging from other, less aggressive, strains (Trotel-Aziz et al., 2022). Since purified (-)-terremutin was not found to be phytotoxic, it might enhance the effect of other factors needed for apoplexy. Thus, the presence of effectors is not sufficient to constitute a subsequent evolutionary development towards biotrophy but must involve additional changes—these might be mechanisms to promote hyphal invasiveness. In fact, there are differences in the cell biology of endophytic versus pathogenic growth phases. Endophytes grow by intercalation (Christensen et al., 2008), the polar growth at the hyphal tip is a necessary condition for pathogenicity whatever fungal pathogen lifestyle (Brand & Gow, 2009). A recent study on the secretome of *N. parvum* hosted by Eucalyptus demonstrated that, in addition to enzymes degrading different components of the plant cell wall, other protein effectors such as chitin modifying enzymes were secreted (Nazar Pour et al., 2022), and suspected that they might both help the fungus to escape detection by host receptors, but also change the cell-wall properties and, thus, the mode of hyphal growth. Similar to other wood-decaying fungi *N. parvum* can feed on cell walls of the xylem parenchyma cell, but also use xylem vessels for long-distance colonisation (Pouzoulet et al., 2022).

Thus, 4-HPA might be a signal that helps foraging local cell-wall resources during the endophytic phase, acting through two very specific mechanisms: by silencing GH3, the fungus would increase steady-state levels of the auxin IAA, leading to increased cell-wall extensibility facilitating foraging cell-wall components, by silencing STS27 and piceatannol, which is generated from feruloyl-CoA (Raiber et al., 1995), such that ferulic acid would be channelled towards monolignols rather than being recruited for phytoalexins.

4.5 | Outlook

Our study identifies 4-hydroxyphenylacetic acid (4-HPA) as a chemical signal that enables a non-pathogenic interaction between *N. parvum* and *Vitis* during the endophytic phase of the *N. parvum*. 4-HPA secretion is halted by the accumulation of the plant surrender signal ferulic acid, which activates the fungal secretion of Fusiccocin A leading to PCD and the possible apoplectic breakdown of the infected host plant (Khattab et al., 2022). Since 4-HPA specifically inhibits *STS27* and prevents the formation of piceatannol, the substrate specificity of this stilbene synthase isotype might be a key for understanding this tactical turn of chemical warfare, for instance by testing recombinantly expressed *STS27* for its ability to convert feruloyl-CoA into piceatannol. Why the other *STS* isoforms seem not targeted by 4-HPA remains another open question and might hint to other mechanisms of escape, for instance by fungal metabolisation (Stempien et al., 2017). In the current and preceding work (Khattab et al., 2022), we demonstrate that the interaction between *N. parvum* and grapevine is orchestrated by chemical interactions that depend on the stress status of the plant, opening new paths to better understand BD development in plants that are challenged by climate-born abiotic stress, aiming towards the development of better biocontrol strategies against BD pathogens. If we succeed to constrain the accumulation of ferulic acid, either by improving the channelling towards piceatannol, or by promoting the conversion into monolignols, maybe the switch to a necrotrophic lifestyle of *N. parvum* could be reduced, mitigating the economic burden due to BD. Another potential strategy might be to apply 4-HPA to plants suffering from climate stress, to inhibit the switch to necrotrophy. Alternatively, approaches preventing the accumulation of ferulic acid, and thus avoiding the plant signal activating the fungal secretion of the phytotoxin FCA, might also help to suppress BD symptom expression.

ACKNOWLEDGEMENTS

The authors want to thank Mr. Kevin Malakowsky for raising the plants for the infection experiment. This work was supported by European Fund for Regional Development (Interreg Upper Rhine, project DialogProTec) and the Strategy Fund of the KIT (project M4F). I.M.K. was awarded also a full PhD scholarship from the German Egyptian Research Long-term Scholarships DAAD-GERLS programme and a DAAD-STIBET scholarship. Open Access funding enabled and organized by Projekt DEAL.

CONFLICT OF INTEREST STATEMENT

The authors declare no conflict of interest.

DATA AVAILABILITY STATEMENT

The data that support the findings of this study are available from the corresponding author upon reasonable request.

ORCID

Noemi Flubacher http://orcid.org/0000-0002-2566-8678
Philippe Hugueney http://orcid.org/0000-0002-1641-9274
Peter Nick http://orcid.org/0000-0002-0763-4175

REFERENCES

Abou-Mansour, E., Débieux, J.-L., Ramírez-Suero, M., Bénard-Gellon, M., Magnin-Robert, M., Spagnolo, A. et al. (2015) Phytotoxic metabolites from *Neofusicoccum parvum*, a pathogen of Botryosphaeria dieback of grapevine. *Phytochemistry*, 115, 207–215.

Adrian, M. & Jeandet, P. (2012) Effects of resveratrol on the ultrastructure of *Botrytis cinerea* conidia and biological significance in plant/pathogen interactions. *Fitoterapia*, 83, 1345–1350.

Akaberi, S., Wang, H., Claudel, P., Riemann, M., Hause, B., Hugueney, P. et al. (2018) Grapevine fatty acid hydroperoxide lyase generates actin-disrupting volatiles and promotes defence-related cell death. *Journal of Experimental Botany*, 69, 2883–2896.

Altschul, S.F., Gish, W., Miller, W., Myers, E.W. & Lipman, D.J. (1990) Basic local alignment search tool. *Journal of Molecular Biology*, 215, 403–410.

Aoi, Y., Tanaka, K., Cook, S.D., Hayashi, K.-I. & Kasahara, H. (2020) GH3 auxin-amido synthetases alter the ratio of indole-3-acetic acid and phenylacetic acid in arabidopsis. *Plant and Cell Physiology*, 61, 596–605.

de Bary, A. (1866) *Morphologie und physiologie der pilze, flechten, und myxomyceten: Hofmeister's Handbook of Physiological Botany*. Leipzig, Germany: Engelmann.

Benjamini, Y. & Hochberg, Y. (1995) Controlling the false discovery rate: a practical and powerful approach to multiple testing. *Journal of the Royal Statistical Society: Series B (Methodological)*, 57, 289–300.

Bertsch, C., Ramírez-Suero, M., Magnin-Robert, M., Larignon, P., Chong, J., Abou-Mansour, E. et al. (2013) Grapevine trunk diseases: complex and still poorly understood. *Plant Pathology*, 62, 243–265.

Blodgett, J.T., Kruger, E.L. & Stanosz, G.R. (1997) *Sphaeropsis sapinea* and water stress in a red pine plantation in Central Wisconsin. *Phytopathology®*, 87, 429–434.

Brand, A. & Gow, N.A. (2009) Mechanisms of hypha orientation of fungi. *Current Opinion in Microbiology*, 12, 350–357.

Buckel, I., Andernach, L., Schüffler, A., Piepenbring, M., Opatz, T. & Thines, E. (2017) Phytotoxic dioxolanones are potential virulence factors in the infection process of *Guignardia bidwellii*. *Scientific Reports*, 7, 8926.

Çakir, B., Kiliçkaya, O. & Olcay, A.C. (2012) Genome-wide analysis of Aux/IAA genes in *Vitis vinifera*: cloning and expression profiling of a grape Aux/IAA gene in response to phytohormone and abiotic stresses. *Acta Physiologiae Plantarum*, 55, 115.

Chang, X., Riemann, M., Liu, Q. & Nick, P. (2015) Actin as deathly switch? How auxin can suppress cell-death related defence. *PLoS One*, 10, e0125498.

Chang, X., Seo, M., Takebayashi, Y., Kamiya, Y., Riemann, M. & Nick, P. (2017) Jasmonates are induced by the PAMP flg22 but not the cell death-inducing elicitor harpin in *Vitis rupestris*. *Protoplasma*, 254, 271–283.

Chong, J., Poutaraud, A. & Hugueney, P. (2009) Metabolism and roles of stilbenes in plants. *Plant Science*, 177, 143–155.

Christensen, M.J., Bennett, R.J., Ansari, H.A., Koga, H., Johnson, R.D., Bryan, G.T. et al. (2008) *Epichloë* endophytes grow by intercalary hyphal extension in elongating grass leaves. *Fungal Genetics and Biology*, 45, 84–93.

Cook, S.D., Nichols, D.S., Smith, J., Chourey, P.S., McAdam, E.L., Quittenden, L. et al. (2016) Auxin biosynthesis: are the indole-3-acetic acid and phenylacetic acid biosynthesis pathways mirror images? *Plant Physiology*, 171, 1230–1241.

Cook, S.D. & Ross, J.J. (2016) The auxins, IAA and PAA, are synthesized by similar steps catalyzed by different enzymes. *Plant Signaling & Behavior*, 11, e1250993.

Delaye, L., García-Guzmán, G. & Heil, M. (2013) Endophytes versus biotrophic and necrotrophic pathogens—are fungal lifestyles evolutionarily stable traits? *Fungal Diversity*, 60, 125–135.

Desprez-Loustau, M.-L., Marçais, B., Nageleisen, L.-M., Piou, D. & Vannini, A. (2006) Interactive effects of drought and pathogens in forest trees. *Annals of Forest Science*, 63, 597–612.

Doyle, J.J. & Doyle, J.L. (1987) A rapid DNA isolation procedure from small quantities of fresh leaf tissues. *Phytochemical Bulletin*, 19, 11–15.

Du, P., Wang, J., He, Y., Zhang, S., Hu, B., Xue, X. et al. (2021) AtFH14 crosslinks actin filaments and microtubules in different manners. *Biology of the Cell*, 113, 235–249.

Duan, D., Halter, D., Baltenweck, R., Tisch, C., Tröster, V., Kortekamp, A. et al. (2015) Genetic diversity of stilbene metabolism in *Vitis sylvestris*. *Journal of Experimental Botany*, 66, 3243–3257.

Eggenberger, K., Sanyal, P., Hundt, S., Wadhwani, P., Ulrich, A.S. & Nick, P. (2017) Challenge integrity: the cell-penetrating peptide BP100 interferes with the auxin-actin oscillator. *Plant & Cell Physiology*, 58, 71–85.

Gaff, D.F. & Okong'o-Ogola, O. (1971) The use of non-permeating pigments for testing the survival of cells. *Journal of Experimental Botany*, 22, 756–758.

Galarneau, E.R.A., Lawrence, D.P., Travadon, R. & Baumgartner, K. (2019) Drought exacerbates Botryosphaeria dieback symptoms in grapevines and confounds host-based molecular markers of infection by *Neofusicoccum parvum*. *Plant Disease*, 103, 1738–1745.

Guan, P., Shi, W., Riemann, M. & Nick, P. (2021) Dissecting the membrane-microtubule sensor in grapevine defence. *Horticulture Research*, 8, 260.

Guan, P., Terigele, G., Schmidt, F., Riemann, M., Fischer, J., Thines, E. et al. (2020) Hunting modulators of plant defence: the grapevine trunk disease fungus *Eutypa lata* secretes an amplifier for plant basal immunity. *Journal of Experimental Botany*, 71, 3710–3724.

Guan, X., Buchholz, G. & Nick, P. (2014) Actin marker lines in grapevine reveal a gatekeeper function of guard cells. *Journal of Plant Physiology*, 171, 1164–1173.

Guan, X., Buchholz, G. & Nick, P. (2015) Tubulin marker line of grapevine suspension cells as a tool to follow early stress responses. *Journal of Plant Physiology*, 176, 118–128.

Guan, X., Essakhi, S., Laloue, H., Nick, P., Bertsch, C. & Chong, J. (2016) Mining new resources for grape resistance against botryosphaeriaceae: a focus on *Vitis vinifera* subsp. sylvestris. *Plant Pathology*, 65(2), 273–284.

Hedenström, E., Fagerlund Edfeldt, A., Edman, M. & Jonsson, B.-G. (2016) Resveratrol, piceatannol, and isorhapontigenin from Norway spruce (*Picea abies*) debarking wastewater as inhibitors on the growth of nine species of wood-decaying fungi. *Wood Science and Technology*, 50, 617–629.

Hofstetter, V., Buyck, B., Croll, D., Viret, O., Couloux, A. & Gindro, K. (2012) What if esca disease of grapevine were not a fungal disease? *Fungal Diversity*, 54, 51–67.

Jiao, Y., Xu, W., Duan, D., Wang, Y. & Nick, P. (2016) A stilbene synthase allele from a Chinese wild grapevine confers resistance to powdery mildew by recruiting salicylic acid signalling for efficient defence. *Journal of Experimental Botany*, 67, 5841–5856.

Kaźmierczak, A., Siatkowska, E., Li, R., Bothe, S. & Nick, P. (2022) Kinetin induces microtubular breakdown, cell cycle arrest and programmed cell death in tobacco BY-2 cells. *Protoplasma*, 260(3), 787–806.

Khattab, I.M., Fischer, J., Kaźmierczak, A., Thines, E. & Nick, P. (2022) Ferulic acid is a putative surrender signal to stimulate programmed cell death in grapevines after infection with *Neofusicoccum parvum*. *Plant, Cell & Environment*, 46, 339–358.

Khattab, I.M., Sahi, V.P., Baltenweck, R., Maia-Grondard, A., Hugueney, P., Bieler, E. et al. (2021) Ancestral chemotypes of cultivated grapevine with resistance to botryosphaeriaceae-related dieback allocate metabolism towards bioactive stilbenes. *New Phytologist*, 229, 1133–1146.

Larach, A., Torres, C., Riquelme, N., Valenzuela, M., Salgado, E., Seeger, M. et al. (2020) Yield loss estimation and pathogen identification from Botryosphaeria dieback in vineyards of central Chile over two growing seasons. *Phytopathologia Mediterranea*, 59, 537–548.

Leal, C., Richet, N., Guise, J.F., Gramaje, D., Armengol, J., Fontaine, F. et al. (2021) Cultivar contributes to the beneficial effects of *Bacillus subtilis* PTA-271 and *Trichoderma atroviride* SC1 to protect grapevine against *Neofusicoccum parvum*. *Frontiers in Microbiology*, 12, 16.

Li, J., Cao, L. & Staiger, C.J. (2017) Capping protein modulates actin remodeling in response to reactive oxygen species during plant innate immunity. *Plant Physiology*, 173, 1125–1136.

Livak, K.J. & Schmittgen, T.D. (2001) Analysis of relative gene expression data using real-time quantitative PCR and the $2^{-\Delta\Delta C}{}_{T}$ method. *Methods*, 25, 402–408.

Maor, R. & Shirasu, K. (2005) The arms race continues: battle strategies between plants and fungal pathogens. *Current Opinion in Microbiology*, 8, 399–404.

Martin, I.R., Vigne, E., Velt, A., Hily, J.-M., Garcia, S., Baltenweck, R. et al. (2021) Severe stunting symptoms upon nepovirus infection are reminiscent of a chronic hypersensitive-like response in a perennial woody fruit crop. *Viruses*, 13, 2138.

Masi, M., Reveglia, P., Femina, G., Baaijens-Billones, R., Savocchia, S. & Evidente, A. (2021) Luteoethanones A and B, two phytotoxic 1-substituted ethanones produced by *Neofusicoccum luteum*, a causal agent of botryosphaeria dieback on grapevine. *Natural Product Research*, 35, 4542–4549.

Mondello, V., Songy, A., Battiston, E., Pinto, C., Coppin, C., Trotel-Aziz, P. et al. (2018) Grapevine trunk diseases: a review of fifteen years of trials for their control with chemicals and biocontrol agents. *Plant Disease*, 102, 1189–1217.

Muller, H.J. (1964) The relation of recombination to mutational advance. *Mutation Research/Fundamental and Molecular Mechanisms of Mutagenesis*, 1, 2–9.

Naseem, M., Kaltdorf, M. & Dandekar, T. (2015) The nexus between growth and defence signalling: auxin and cytokinin modulate plant immune response pathways. *Journal of Experimental Botany*, 66, 4885–4896.

Navarro, L., Dunoyer, P., Jay, F., Arnold, B., Dharmasiri, N., Estelle, M. et al. (2006) A plant miRNA contributes to antibacterial resistance by repressing auxin signaling. *Science*, 312, 436–439.

Nazar Pour, F., Pedrosa, B., Oliveira, M., Fidalgo, C., Devreese, B., Driessche, G.V. et al. (2022) Unveiling the secretome of the fungal plant pathogen *Neofusicoccum parvum* induced by in vitro host mimicry. *Journal of Fungi*, 8, 971.

Nick, P., Han, M.-J. & An, G. (2009) Auxin stimulates its own transport by shaping actin filaments. *Plant Physiology*, 151, 155–167.

Parage, C., Tavares, R., Réty, S., Baltenweck-Guyot, R., Poutaraud, A., Renault, L. et al. (2012) Structural, functional, and evolutionary analysis of the unusually large stilbene synthase gene family in grapevine. *Plant Physiology*, 160, 1407–1419.

Pouzoulet, J., Yelle, D.J., Theodory, B., Nothnagel, E.A., Bol, S. & Rolshausen, P.E. (2022) Biochemical and histological insights into the interaction between the canker pathogen *Neofusicoccum parvum* and *Prunus dulcis*. *Phytopathology*®, 112, 345–354.

Qiao, F., Chang, X.-L. & Nick, P. (2010) The cytoskeleton enhances gene expression in the response to the harpin elicitor in grapevine. *Journal of Experimental Botany*, 61, 4021–4031.

Raiber, S., Schröder, G. & Schröder, J. (1995) Molecular and enzymatic characterization of two stilbene synthases from eastern White pine (*Pinus strobus*) A single Arg/His difference determines the activity and the pH dependence of the enzymes. *FEBS Letters*, 361, 299–302.

Ramírez-Suero, M., Bénard-Gellon, M., Chong, J., Laloue, H., Stempien, E., Abou-Mansour, E. et al. (2014) Extracellular compounds produced by fungi associated with botryosphaeria dieback induce differential defence gene expression patterns and necrosis in *Vitis vinifera* cv. chardonnay cells. *Protoplasma*, 251, 1417–1426.

Reis, P., Magnin-Robert, M., Nascimento, T., Spagnolo, A., Abou-Mansour, E., Fioretti, C. et al. (2016) Reproducing botryosphaeria dieback foliar symptoms in a simple model system. *Plant Disease*, 100, 1071–1079.

Reveglia, P., Savocchia, S., Billones-Baaijens, R., Masi, M., Cimmino, A. & Evidente, A. (2019) Phytotoxic metabolites by nine species of botryosphaeriaceae involved in grapevine dieback in Australia and identification of those produced by *Diplodia mutila*, *Diplodia seriata*, *Neofusicoccum australe* and *Neofusicoccum luteum*. *Natural Product Research*, 33, 2223–2229.

Ridgway, H.J., Amponsah, N.T., Brown, D.S., Baskarathevan, J., Jones, E.E. & Jaspers, M.V. (2011) Detection of botryosphaeriaceous species in environmental samples using a multi-species primer pair. *Plant Pathology*, 60, 1118–1127.

Salvatore, M.M., Alves, A. & Andolfi, A. (2021) Secondary metabolites produced by *Neofusicoccum* species associated with plants: a review. *Agriculture (London)*, 11, 149.

Schoeneweiss, D.F. (1981) The role of environmental stress in diseases of woody plants. *Plant Disease*, 65, 308.

Slippers, B. & Wingfield, M.J. (2007) Botryosphaeriaceae as endophytes and latent pathogens of woody plants: diversity, ecology and impact. *Fungal Biology Reviews*, 21, 90–106.

Smertenko, A. & Franklin-Tong, V.E. (2011) Organisation and regulation of the cytoskeleton in plant programmed cell death. *Cell Death & Differentiation*, 18, 1263–1270.

Sosnowski, M.R., Luque, J., Loschiavo, A., Martos, S., García-Figueres, F., Wicks, T. et al. (2011) Studies on the effect of water and temperature stress on grapevines inoculated with *Eutypa lata*. *Phytopathologia Mediterranea*, 50, 127–138.

Stempien, E., Goddard, M.-L., Wilhelm, K., Tarnus, C., Bertsch, C. & Chong, J. (2017) Grapevine Botryosphaeria dieback fungi have specific aggressiveness factor repertory involved in wood decay and stilbene metabolization. *PLoS One*, 12, e0188766.

Sugawara, S., Mashiguchi, K., Tanaka, K., Hishiyama, S., Sakai, T., Hanada, K. et al. (2015) Distinct characteristics of indole-3-acetic acid and phenylacetic acid, two common auxins in plants. *Plant and Cell Physiology*, 56, 1641–1654.

Svyatyna, K., Jikumaru, Y., Brendel, R., Reichelt, M., Mithöfer, A., Takano, M. et al. (2014) Light induces jasmonate-isoleucine conjugation via OsJAR1-dependent and -independent pathways in rice. *Plant, Cell & Environment*, 37, 827–839.

Tan, X., Calderon-Villalobos, L.I.A., Sharon, M., Zheng, C., Robinson, C.V., Estelle, M. et al. (2007) Mechanism of auxin perception by the TIR1 ubiquitin ligase. *Nature*, 446, 640–645.

Tian, M., Chaudhry, F., Ruzicka, D.R., Meagher, R.B., Staiger, C.J. & Day, B. (2009) Arabidopsis actin-depolymerizing factor AtADF4 mediates defense signal transduction triggered by the *Pseudomonas syringae* effector AvrPphB. *Plant Physiology*, 150, 815–824.

Trotel-Aziz, P., Abou-Mansour, E., Courteaux, B., Rabenoelina, F., Clément, C., Fontaine, F. et al. (2019) Bacillus subtilis PTA-271 counteracts Botryosphaeria dieback in grapevine, triggering immune responses and detoxification of fungal phytotoxins. *Frontiers in Plant Science*, 10, 25.

Trotel-Aziz, P., Robert-Siegwald, G., Fernandez, O., Leal, C., Villaume, S., Guise, J.-F. et al. (2022) Diversity of *Neofusicoccum parvum* for the production of the phytotoxic metabolites (-)-terremutin and (R)-mellein. *Journal of Fungi*, 8, 319.

Úrbez-Torres, J.R. (2011) The status of Botryosphaeriaceae species infecting grapevines. *Phytopathologia Mediterranea*, 50, 5–45.

Úrbez-Torres, J.R. & Gubler, W.D. (2009) Pathogenicity of Botryosphaeriaceae species isolated from grapevine cankers in California. *Plant Disease*, 93, 584–592.

Wang, H., Riemann, M., Liu, Q., Siegrist, J. & Nick, P. (2021) Glycyrrhizin, the active compound of the TCM drug *Gan Cao* stimulates actin remodelling and defence in grapevine. *Plant Science*, 302, 110712.

Wang, L. & Nick, P. (2017) Cold sensing in grapevine – which signals are upstream of the microtubular "thermometer". *Plant, Cell & Environment*, 40, 2844–2857.

Wang, R., Duan, D., Metzger, C., Zhu, X., Riemann, M. & Pla, M. et al. (2022) Aluminum can activate grapevine defense through actin remodeling. *Horticulture Research*, 9, uhab016.

Wightman, F. & Lighty, D.L. (1982) Identification of phenylacetic acid as a natural auxin in the shoots of higher plants. *Physiologia Plantarum*, 55, 17–24.

Wilson, D. (1995) Endophyte: the evolution of a term, and clarification of its use and definition. *Oikos*, 73, 274.

SUPPORTING INFORMATION

Additional supporting information can be found online in the Supporting Information section at the end of this article.

How to cite this article: Flubacher, N., Baltenweck, R., Hugueney, P., Fischer, J., Thines, E., Riemann, M. et al. (2023) The fungal metabolite 4-hydroxyphenylacetic acid from *Neofusicoccum parvum* modulates defence responses in grapevine. *Plant, Cell & Environment*, 1–17. https://doi.org/10.1111/pce.14670